The Astrophysical Journal, 625:563–574, 2005 May 20

COMPARISON OF RADIATIVE ACCELERATIONS OBTAINED WITH ATOMIC DATA FROM OP AND OPAL

Franck Delahaye[1,2] and Marc Pinsonneault[1]
Received 2004 November 30; accepted 2005 February 7

ABSTRACT

Microscopic diffusion processes (such as radiative levitation, gravitational settling, and thermal diffusion) in the outer layers of stars are important because they may give rise to surface abundance anomalies. Here we compare radiative accelerations ($g_{\rm rad}$) derived from the new Opacity Project (OP) data with those computed from OPAL and some previous data from OP. For the case in which we have full data from OPAL (carbon, five points in the ρ-T plane), the differences in the Rosseland mean opacities between OPAL and the new OP data are within 12% and are less than 30% between new OP and previous OP data (OP1). The radiative accelerations $g_{\rm rad}$ differ at up to the 17% level when compared to OPAL and up to the 38% level when compared to OP1. The comparison with OP1 on a larger ρ-T space gives a difference of up to 40% for $g_{\rm rad}$(C) and increases for heavier elements, reaching 60% for Si and 65% for S and Fe. We also constructed four representative stellar models in order to compare the new OP accelerations with prior published results that used OPAL data. The Rosseland means overall agree better than 10% for all our cases. For the accelerations, the comparisons with published values yield larger differences in general. The published OPAL accelerations for carbon are even larger relative to OP compared to those that our direct comparisons indicate. Potential reasons for this puzzling behavior are discussed. In light of the significant differences in the inferred acceleration rates, theoretical errors should be taken into account when comparing models with observations. The implications for stellar evolution are briefly discussed. The sensitivity of $g_{\rm rad}$ to the atomic physics may provide a useful test of different opacity sources.

Subject headings: atomic data — stars: evolution — stars: interiors

Online material: color figures

1. INTRODUCTION

Element segregation processes are clearly seen in stars and solar models and occur from well-understood physical processes. Gravitational settling and thermal diffusion tend to make heavier species sink relative to light ones. Radiative pressure tends to cause some species to rise in the stellar interior (we refer to this as radiative acceleration). Radiative accelerations have been calculated using the Opacity Project (OP; Seaton et al. 1994, 1995, 1997) data (Alecian & Artru 1990; Alecian et al. 1993; Alecian 1994; Gonzalez et al. 1995; LeBlanc & Michaud 1995; Hui-Bon-Hoa et al. 1996; Seaton 1997, 1999; Alecian & LeBlanc 2000; LeBlanc & Alecian 2004).[3] Evolutionary calculations, however, have almost all been based on the OPAL theoretical opacities (Iglesias & Rogers 1996), except for those of Seaton (1999).

In this paper we compare results from the updated data from OP with those obtained from OPAL and previous data from OP. We begin by discussing the astrophysical impact of element separation processes and then move to our motivation for comparing with other data sets.

It is now generally accepted, as proposed by Michaud (1970) for Ap stars and Watson (1970) for AmFm stars, that radiative levitation plays an important role in hot and slow-rotating stars. The morphology of the horizontal branches (HBs) of different globular clusters (GCs) presents some features that are not predicted by standard stellar models: gaps in the blue tail (Ferraro et al. 1998), jumps in the Strömgren color-magnitude diagram (Grundahl et al. 1999), surface gravity anomalies (Moehler et al. 1995), and abundance anomalies (Behr et al. 1999, 2000a, 2000b). This results in a bimodal distribution in the HB stars of the studied GCs. Qualitatively, Hui-Bon-Hoa et al. (2000) showed that these observations could be the signatures of radiative acceleration ($g_{\rm rad}$).

Microscopic diffusion can also affect the internal structure of stars. The impact of gravitational settling on solar models has been extensively explored (Bahcall & Pinsonneault 1992, 1995; Vauclair 1998; Turck-Chiéze et al. 1998; Sackmann & Boothroyd 2003). Diffusion deepens the solar surface convection zone, improving the agreement with helioseismic data on its depth, and yields a surface helium abundance in good agreement with the value deduced from helioseismic studies. Element separation processes affect the thermal structure, the convection depth, and the inferred initial abundances of solar models (Charpinet et al. 1997; Turcotte et al. 1998a, hereafter T98a; Turcotte et al. 1998b, hereafter T98b; Richer et al. 1998, hereafter R98).

In addition, GC age estimates are affected by the inclusion of settling and diffusion (Chaboyer et al. 1992a, 1992b; VandenBerg et al. 2002), leading to an age reduction of order 10% relative to models that neglect settling. Michaud et al. (2004) showed the importance of microdiffusion in the age determination of open clusters and its effect on isochrone morphology. It has become clear that radiative levitation and diffusion processes must be included in stellar evolution codes in a self-consistent manner.

Computing these effects has been challenging; detailed comparisons between theory and observations have had mixed success. T98a found that their predicted overabundances were larger than the observed ones. They explored other physical processes, such as turbulent diffusion and mass loss (T98a; Richer et al. 2000), as potential solutions. However, it is also possible that the uncertainties in the diffusion velocities themselves could be a

[1] Department of Astronomy, Ohio State University, Columbus, OH 43210.
[2] Observatoire de Paris, LUTH, CNRS UMR 8102 and Université Paris 7, 5 place Jules Janssen, F-92195 Meudon, France.
[3] These data will be made generally available via a server or on CD-ROM. All requests should be sent to Claude Zeippen (Claude.Zeippen@obspm.fr) or Anil Pradhan (pradhan@astronomy.ohio-state.edu).

significant error source. Because the two effects (gravitational settling and levitation) are in opposite senses, a small difference in the radiative acceleration could change the magnitude (or even the sign) of the predicted abundance anomalies by a much larger than linear factor when the two effects are of similar magnitude. Before any attempt to generate a model with microdiffusion including radiative levitation, a careful study of the atomic data available is necessary. We therefore evaluate the uncertainties in the radiative acceleration coefficients themselves.

In § 2 we describe the method used to obtain the radiative accelerations and the different stellar model structures. In § 3.1 we compare and analyze the results from the new data (NEW) and from the previous OP data. In § 3.2 we compare the results from OPAL and NEW for carbon. This is the only element for which we have some monochromatic opacities from OPAL. For the other elements, we compare our results with published works in § 3.3. The discussion and the conclusion constitute §§ 4 and 5, respectively.

2. METHOD

In a star, the net radiative flux goes outward. As the photons move toward the surface, they interact with the ions present in the star. Each species, depending on its state of ionization, its excitation level, and its corresponding absorption cross section, experiences a net force that tends to make ions rise when they absorb momentum from photons. The resulting acceleration is called the radiative acceleration and is defined as follows (Seaton 1997):

$$g_{\rm rad}(k) = \frac{F}{c}\frac{M}{M(k)}\kappa_{\rm R}\gamma(k), \tag{1}$$

where M is the mean mass per atom, $M(k)$ is the atomic mass of atom k, $\kappa_{\rm R}$ is the Rosseland mean, F is the total flux of the radiative source (a blackbody at $T = T_{\rm eff}$), and F/c is the total momentum radiative flux associated with it. Finally, $\gamma(k)$ is a dimensionless quantity characterizing the individual contribution of element k to the total opacity, defined as follows (Seaton 1997):

$$\gamma(k) = \int \frac{\kappa_\nu(k)}{\kappa_\nu({\rm tot})} f_\nu \, d\nu, \tag{2}$$

$$\kappa_\nu({\rm tot}) = \sum_k \kappa_\nu(k) + \kappa_{\rm scat}, \tag{3}$$

where $\kappa_\nu(k)$ is the monochromatic opacity of element k and $\kappa_\nu({\rm tot})$ is the total opacity, both in units of cm^2 g^{-1} of the mixture, and f_ν is a weighting function defined below. As a reminder, with this notation, $\kappa_{\rm R}$ is defined as

$$\frac{1}{\kappa_{\rm R}} = \int \frac{1}{\kappa_\nu({\rm tot})} f_\nu \, d\nu, \tag{4}$$

$$f_\nu = \frac{15h^5\nu^4}{4\pi^4 k_{\rm B}^5 T^5}\frac{e^{h\nu/k_{\rm B}T}}{(e^{h\nu/k_{\rm B}T}-1)^2}. \tag{5}$$

In the present work, we compute $g_{\rm rad}$ both with and without including the effect of momentum transfer to electrons during photoionization processes. In other words, we have used $\kappa_\nu(k)$ or $\kappa_\nu^{\rm mta}(k)$ (as defined in eq. [31] of Seaton [1997]). This allows us to isolate each difference in the atomic data. For the OPAL data, as for the OP data, we subtracted the electron scattering opacities and the opacities corresponding to the momentum transferred to the electrons during the photoionization from the monochromatic opacities of the studied elements. However, this is not subtracted from the total opacity. We used exclusively the OP data to remove these contributions. We did not remove the OPAL electron scattering opacity from the OPAL data because it is already subtracted via the OP data.

TABLE 1
Comparison of Monochromatic and Total Opacities in the ρ-T Plane

Point	log T	log R	log ρ
1	6.0	−1.5	−1.5
2	6.0	−2.0	−2.0
3	6.0	−2.5	−2.5
4	6.0	−3.0	−3.0
5	6.3	−1.5	−0.6

Note.—For reference, at the base of the solar convection zone in our model, log $T = 6.33$ and log $\rho = -0.735$.

In order to estimate the systematic errors in the radiative accelerations due to atomic data, we compare the values of $g_{\rm rad}$ obtained with four sets of atomic data, two from OPAL and two from OP (NEW and OP1).[4] We compare with OPAL data for carbon (C. Iglesias 2004, private communication) at the five points in the ρ-T plane listed in Table 1 and discuss indirect comparisons with the literature in § 3. Ideally, one would directly compare the monochromatic opacities (total and specific for each element) from OP and OPAL. However, because of technical problems the OPAL group could not provide a full set of data.

We first calculated the Rosseland mean opacities and γ(C) with the three sets of data. We then calculated the accelerations for different sets of $T_{\rm eff}$ and radius (these determine the flux in eq. [1]).

For the other elements present in the mixture, we do not have the relevant OPAL atomic data. In § 3.2 we thus compare OP data for other elements with previously published OPAL results (T98a, T98b; R98). We calculated the Rosseland mean opacities, the values of $\gamma(k)$, and the radiative accelerations using OP data for different types of stars. This indirect comparison allows us to span a large portion of the ρ-T plane. As we will show, however, it is difficult to directly interpret differences obtained in this manner.

We calculate the structure of different stars with the YREC code (see Bahcall et al. [2001] for a description of the model ingredients), in which we modified the microdiffusion subroutines. We extended the composition vector to include all species present in the mixture in order to track individually their evolution within the model as a function of time. The diffusion equation for element separation processes has been modified in order to treat each species of the initial mixture separately. Instead of treating the gravitational accelerations of all elements as if they were settling like fully ionized Fe, the gravitational settling coefficients are calculated individually for each element. We also included the individual radiative accelerations calculated using the OP data and the method described by Seaton (1997, 1999). All the technical details of the calculation will be presented in a subsequent paper.

We first calibrated our model with a mass of 1.0 $M_\odot$ to reproduce the observed solar luminosity ($L_\odot$), radius ($R_\odot$), and surface Z/X ratio at the solar age (4.57 Gyr). The initial composition used here includes 17 elements (H, He, C, N, O, Ne, Na, Mg, Al, Si, S, Ar, Ca, Cr, Mn, Fe, and Ni) with relative abundances from the Grevesse & Noel (1993) mixture. The calibrated model yields

[4] The OP1 data are those in the database at the Centre de Données de Strasbourg (CDS; http://cdsweb.u-strasbg.fr).

TABLE 2
Compositions Used in Modeling

Element	Z	Number Fraction
H	1	9.071E−01
He	2	9.135E−02
C	6	3.770E−04
N	7	9.913E−05
O	8	7.877E−04
Ne	10	1.277E−04
Na	11	2.271E−06
Mg	12	4.039E−05
Al	13	3.135E−06
Si	14	3.769E−05
S	16	1.722E−05
Ar	18	3.518E−06
Ca	20	2.434E−06
Cr	24	5.047E−07
Mn	25	2.608E−07
Fe	26	3.359E−05
Ni	28	1.985E−06

the initial helium mass fraction ($Y_\odot = 0.271$) and the mixing length ($\alpha_0 = 2.09$). We used this solar calibration for our other models. As previously noted (T98b), it might not be justified to use these parameters from a calibrated Sun for stars with a range of masses and evolutionary states. However, by doing so we transform the absolute errors in the input physics into relative ones, which is a significant advantage for a solar calibration. For all models, as well as for the five special points for which we have the monochromatic opacities from OPAL, we used the composition given in Table 2.

In the present work we focus primarily on quantifying the errors in the coefficients themselves, so we have not yet included the feedback on the opacity induced by changes in the heavy-element mixture. Changes in the relative heavy-element abundances can certainly be important in some contexts, as suggested by Alecian et al. (1993). For example, Richer et al. (2000) found an iron convection zone in AmFm models including microdiffusion that was caused by feedback effects. We intend to include such effects in future work focused on the applications of diffusion to stellar evolution problems.

3. RESULTS

Our aim in this section is twofold: we present the effect of the updated OP opacities on the radiative acceleration and then compare the new results to OPAL. We present two specific cases, C and Fe, to show how the monochromatic opacities modify the radiative acceleration. The improvement in the OP atomic data due to the inclusion of inner shell transitions systematically enhances the radiative accelerations relative to the older OP data. The impact of the new physics increases for heavier species and higher temperature. When directly compared to the OPAL data, the accelerations for carbon are in reasonable agreement. However, this agreement deteriorates in the comparison with published work. The agreement between OP and OPAL is expected to be, and is, less favorable for heavier elements.

3.1. *Comparison between NEW and OP1*

In order to understand the contribution of different ingredients to $g_{\rm rad}$, we present the monochromatic opacities for C and Fe at a specific ρ-T point. The main difference between the two sets of data (OP1 and NEW) is the inclusion of the inner shell transitions in the latter.

For our purpose, it is worth recalling that the acceleration $g_{\rm rad} \propto \kappa_{\rm R}\gamma$ and $\gamma \propto \int (\kappa_{\rm elem}/\kappa_{\rm tot}) f_\nu \, d\nu$. The interplay between the various terms in equation (1) is illustrated in Figure 1. The data used for this figure are from the new OP data and OP data without inner shell transitions (M. J. Seaton 2004, private communication). Figure 1 (*top*) shows the monochromatic opacities for C (*left*) and Fe (*right*). Figure 1 (*middle*) compares the total monochromatic opacities (same on each side), and Figure 1 (*bottom*) illustrates the ratio of the two, which corresponds to part of the integrand in the definition of γ (see eq. [2]) as a function of u ($u = h\nu/kT$). The physical conditions ($\log T = 6.3$ and $\log R = -1.5$, where R is defined [as in previous OPAL works] as $R = \rho/T_6^3$, with $T_6 = T/10^6$, where ρ is the mass density in g cm^{-3} and T is the temperature in kelvins) correspond to point 5 in Table 1 and are close to the conditions at the base of the convection zone of the Sun. These monochromatic opacities have been obtained by interpolating OP mesh data (OP5 data; M. J. Seaton 2004, private communication) in Ne (electron density corresponding to $\log R = -1.5$). Using these interpolated opacities to calculate $\kappa_{\rm R}$, γ, and $g_{\rm rad}$ generates an error smaller than 2%. We estimate this error by comparing the values of $\kappa_{\rm R}$, γ, and $g_{\rm rad}$ obtained with the interpolated opacities to the values derived from the interpolation of four values of $\kappa_{\rm R}$ (or γ or $g_{\rm rad}$) calculated on the grid point.

From Figure 1 (*top and middle*), one can see that the new OP values are higher than the OP1 values for both the individual and the total monochromatic opacities. However, the increase in the specific elemental opacities is small for C, large for Fe, and intermediate for the total opacities. This arises naturally from the changes in atomic physics. The inner shell transitions included in the new OP data significantly enhanced the Fe monochromatic opacities but led to a small effect for C, as expected (C is almost fully ionized). By definition, γ is governed by the ratio of the individual to the total monochromatic opacities weighted by f_ν. The weighting function f_ν decreases rapidly at low and high frequencies, damping all differences for these regions.

At lower temperatures, the importance of the inner shell decreases, and for the physical conditions typical of envelopes, the two sets of data are in good agreement (within 20%). The previous data were meant to be used for this purpose (Seaton et al. 1994).

In the case of carbon, the differences between the two ratios (NEW and OP1) are reduced when we compare the γ-factors. This can be seen in Figure 1 (*bottom left*): $\kappa_\nu^{\rm OP1} \leq \kappa_\nu^{\rm NEW}$ and $\kappa_{\rm tot}^{\rm OP1} \ll \kappa_{\rm tot}^{\rm NEW}$, but $\kappa_{\rm tot}^{\rm OP1}/\kappa_{\rm tot} < \kappa_{\rm tot}^{\rm NEW}/\kappa_{\rm tot}$.

For carbon, the increase in the total monochromatic opacities reduces significantly. As a consequence, the difference in $g_{\rm rad} \propto \kappa_{\rm R}\gamma$ is smaller than in $\kappa_{\rm R}$. The changes in γ are partially compensated by those in $\kappa_{\rm R}$.

In the case of iron, the fractional changes in the Fe monochromatic opacities are greater than those for $\kappa_{\rm tot}$, which makes γ larger. This makes $g_{\rm rad}$ significantly larger compared to the OP1 values.

We calculated the acceleration for 15 elements present in the mixture for a range of ρ-T values characteristic of the physical conditions found in different stellar models. The details of these models are given later in this section. For all the different structures, $\kappa_{\rm R}$ differs on average by less than 30% (see Table 3), with particular points differing by up to 38% (see Fig. 2). For the acceleration, the results depend on the element, and we can divide them into two groups.

3.1.1. *Light Elements:* C *to* Al

The lighter metals follow the pattern seen in the carbon data. The differences in the acceleration are less than 40%, with an rms

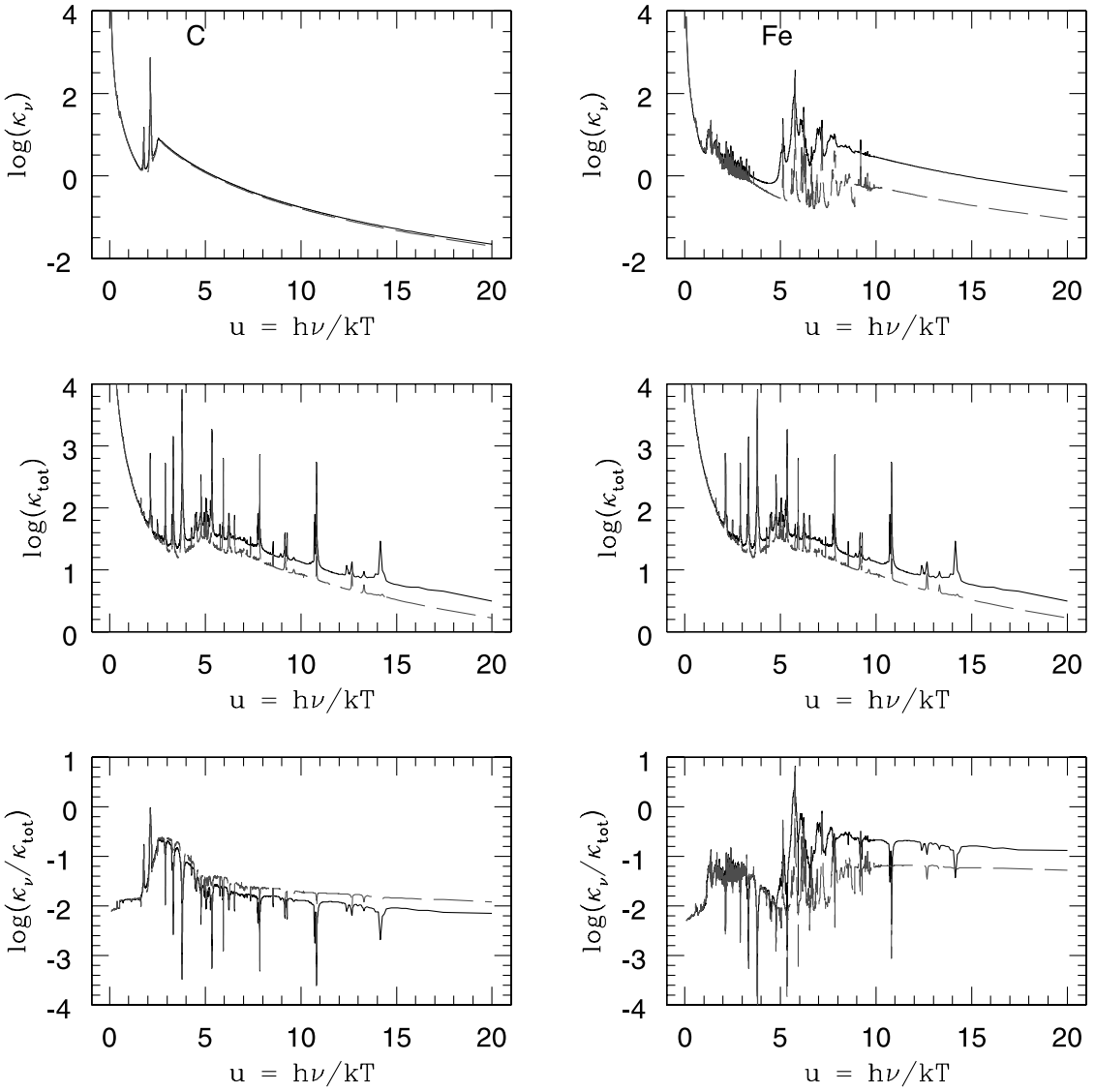

FIG. 1.—Monochromatic opacities at $\log T = 6.3$ and $\log R = -1.5$. *Left*, Carbon; *right*, iron; *top*, monochromatic opacities; *middle*, total opacities; *bottom*, $\kappa_\nu(\mathrm{C})/\kappa_\nu^{\mathrm{tot}}$; *dashed line*, OP1; *solid line*, new OP. [*See the electronic edition of the Journal for a color version of this figure.*]

error smaller than 40%, in the sense that the new data are larger. These differences are dominated by the Rosseland mean, and consequently the global effect is not. The monochromatic opacities for these elements are not significantly modified by the inclusion of the inner shell transitions. The total monochromatic opacities are affected by the other abundant species for which the inner shell transitions are important. As a consequence, the ratio of the two presents a difference that is balanced by the differences in the Rosseland mean opacity. The final results are closer than the Rosseland mean opacities themselves.

TABLE 3

PERCENTAGE DIFFERENCE (rms) FOR ALL POINTS OF EACH MODEL

Model	NEW−OPAL (%)	NEW−OP1 (%)	OPAL−OP1 (%)
Sun at 4.57 Gyr.....	1.3	29	29
$T_{\mathrm{eff}} = 10{,}000$ K.....	6.2	6.5	9.5
$M = 1.3\ M_\odot$.....	1.9	27	26.9
$M = 1.5\ M_\odot$.....	4.8	17.4	17.6

NOTE.—In our models, rms $= [(1/N)\sum(\Delta\kappa_{\mathrm{R}}/\kappa_{\mathrm{R}})^2]^{1/2}$.

3.1.2. *Heavy Species:* Si *to* Ni

For the heavy elements, the accelerations increase by up to 80%, with an rms between 10% and 65%. These elements have two regimes. At lower temperatures, the increase in the monochromatic opacities is of the same order as the total monochromatic opacities, and the ratio of the two, which constitutes the integrand in γ, stays relatively constant. Then the differences in the accelerations follow the trend of κ_{R}, which does not differ a lot between the two data sets. At higher temperatures, where the contribution of the inner shell transitions is very important, the ratio is not similar, and γ differs significantly ($\gamma_{\mathrm{NEW}} > \gamma_{\mathrm{OP1}}$). The increase in the elemental monochromatic opacities is much more important than the rise in the total monochromatic opacities. Here κ_{R} is also larger, resulting in a significant increase in the acceleration.

3.2. *OP and OPAL: Direct Comparison for* C

The monochromatic opacities for carbon obtained from the OPAL group allow us to directly gauge the effect of the difference in atomic data in calculating the radiative accelerations. The OPAL data have been resampled and interpolated in order to match the frequency points used in the OP data. This does not

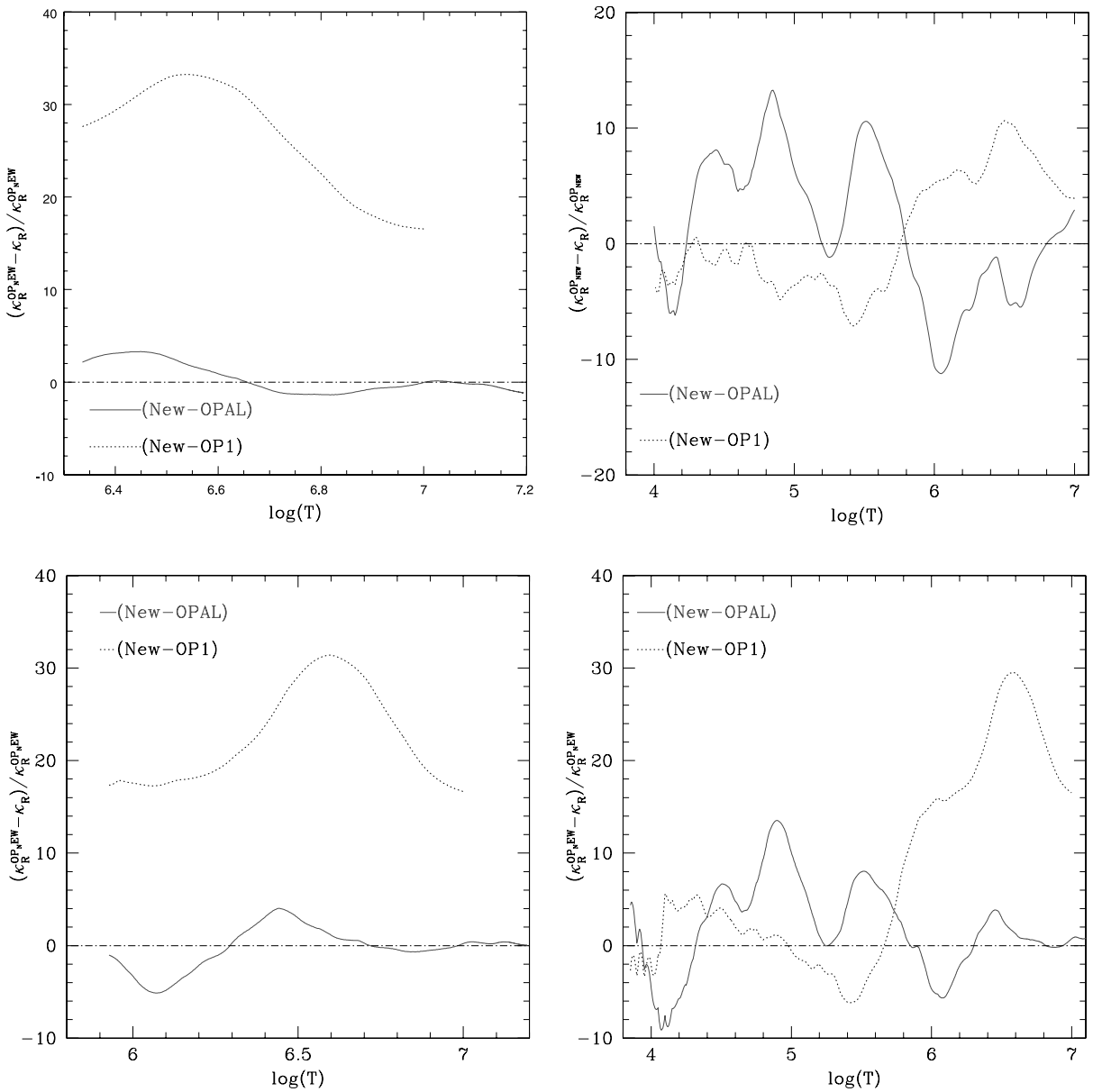

FIG. 2.—Percentage difference in κ_R between OPAL and OP. *Top left*, Sun at 4.57 Gyr; *top right*, $T_{\rm eff} = 10{,}000$ K and $\log R = -3$; *bottom left*, $M = 1.3\ M_\odot$ and $T = 6500$ K; *bottom right*, $M = 1.5\ M_\odot$ and $T = 7070$ K. [*See the electronic edition of the Journal for a color version of this figure*.]

TABLE 4

OPAL AND OP VALUES OF κ_R AND γ_C

$\log T$	$\log \rho$	$\kappa_R^{\rm pres}$	$\kappa_R^{\rm OPAL}$	$\kappa_R^{\rm OP5}$	NEW−OPAL (%)	NEW−OP1 (%)
6.0.....	−1.5	58.75	60.38 (60.37)	44.63	−2.7	24.1
6.0.....	−2.0	27.54	28.83 (28.90)	22.10	−4.7	19.8
6.0.....	−2.5	10.29	11.42 (11.52)	8.93	−10.9	13.2
6.0.....	−3.0	3.41	3.65 (3.72)	3.22	−7.0	5.6
6.3.....	−0.6	34.89	35.79 (35.76)	24.61	−2.6	29.5

NOTE.—The percentage differences correspond to $(\kappa_R^{\rm OP} - \kappa_R^{\rm OPAL})/\kappa_R^{\rm OPAL}$. The OPAL Rosseland mean has been recalculated using a sampling and interpolation procedure in order to have the same frequency point. This procedure has an error of less than 1%, except for point 4 ($\log T = 6.0$ and $\log \rho = -3.0$), for which the difference between the recalculated value (in parentheses) and the value given by OPAL is 1.8%.

TABLE 5
COMPARISON OF γ(C) OBTAINED WITH OPAL AND OP DATA (NEW)

log T	log ρ	log $T_{\rm eff}$	r/R_*	log $\gamma^{\rm NEW}$	log $\gamma^{\rm OPAL}$	$\delta\gamma_1/\gamma$ (%)
6.0.....	−1.5	3.762	0.7146	2.668	2.664	0.9
6.0.....	−2.0	3.762	0.7146	2.583	2.579	0.9
6.0.....	−2.5	3.762	0.7146	2.491	2.476	3.4
6.0.....	−3.0	3.762	0.7146	2.406	2.407	−0.2
6.3.....	−0.6	3.762	0.7146	2.239	2.188	11.1

NOTES.—The effects of momentum transfer to the electron are not taken into account. For this comparison, $\delta\gamma_1/\gamma = (\gamma^{\rm NEW} - \gamma^{\rm OPAL})/\gamma^{\rm NEW}$.

introduce any significant error (less than 2% in all parameters). We estimated this error by recomputing the Rosseland mean opacity and comparing it to the value provided with the data by the OPAL group. In Table 4, the values in parentheses are the recalculated values. We also reproduced Figure 3 from Iglesias & Rogers (1995). We are confident that any errors introduced by this procedure are negligible and allow a fair comparison.

In Table 4 we compare the OP and OPAL Rosseland mean opacity values. The results for the Rosseland mean show a difference that does not exceed 12%, in the sense that the new OP opacities are lower than OPAL (the differences between NEW and OP1 range from 6% to 30%). A detailed discussion on the comparison of Rosseland means can be found in Badnell et al. (2005). In particular, the difference for the solar case is only 2.5%.

The results for γ and $g_{\rm rad}$ are presented in Tables 5–8. The γ(C) factors differ by less than 12% when compared to OPAL and by less than 15% for OP1. The momentum transfer to the electrons does not change the results. The net results on the accelerations range from 5% to 12% when compared to OPAL without the correction for momentum transfer to the electrons and from 2% to 17% when this effect is included. When compared to OP1, the differences are less than 38% with corrections for momentum transfer to the electrons.

3.3. *OP versus OPAL: Other Elements*

The comparison with OPAL for other elements can only be inferred indirectly at the moment. The OPAL atomic data are not available. However, Figures 5, 6, 7, and 10 of Seaton & Badnell (2004) give an insight of the expected differences. For these simple mixtures, one probes the difference of the element's contribution in either data set. As we have shown above, the differences for the carbon monochromatic opacities are small (Seaton & Badnell 2004, Fig. 5). The same results are expected for O (Seaton & Badnell 2004, Fig. 6). The differences increase for S (Seaton & Badnell 2004, Fig. 7) and become significant for Fe (Seaton & Badnell 2004, Fig. 10). All these results are for the conditions of the five points from Table 1. An interesting point is that the new data produce larger monochromatic opacities for C, O, and S compared to OPAL but smaller values for Fe. To extend the comparison, we have calculated the accelerations for different elements for four stellar models and compare them to previous published works.

TABLE 7
COMPARISON OF THE C ACCELERATION OBTAINED WITH OPAL AND OP DATA (NEW)

log T	log ρ	log $T_{\rm eff}$	r/R_*	log $g_{\rm rad}^{\rm NEW}$	log $g_{\rm rad}^{\rm OPAL}$	$\delta g_1/g$ (%)
6.0.....	−1.5	3.762	0.7146	4.077	4.097	−4.7
6.0.....	−2.0	3.762	0.7146	3.664	3.692	−6.7
6.0.....	−2.5	3.762	0.7146	3.145	3.190	−10.9
6.0.....	−3.0	3.762	0.7146	2.580	2.629	−11.9
6.3.....	−0.6	3.762	0.7146	3.423	3.393	6.7

NOTES.—The accelerations do not take into account the effect of momentum transfer to the electron. When the correction is applied, the differences increase. For this comparison, $\delta g_1/g = (g^{\rm NEW} - g^{\rm OPAL})/g^{\rm NEW}$.

3.3.1. *Models*

For the other elements the four types of models used here are as follows:

1. The Sun at 4.57 Gyr;
2. A model (R98) with $T_{\rm eff} = 10{,}000$ K and $\log R = -3$, where R is defined (as in previous OPAL works) as $R = \rho/T_6^3$, with $T_6 = T/10^6$, where ρ is the mass density in g cm^{-3} and T is the temperature in kelvins;
3. An $M = 1.3\ M_\odot$ model at 70 Myr ($T_{\rm eff} = 6500$ K);
4. An $M = 1.5\ M_\odot$ model at 30 Myr ($T_{\rm eff} = 7080$K).

We picked regimes in which the diffusion effects are known to be important. While levitation is a small effect in the Sun, we have precise data to compare theory and observations. The solar models therefore provide a useful point of comparison with other investigators. The other models are in regimes in which radiative levitation is most likely to play an important role; the different cases span a large domain of the ρ-T space. The second case is designed to mimic the physical conditions appropriate for hot HB stars or intermediate main-sequence stars of mass around 2.5 $M_\odot$. The third and fourth cases are models of typical F stars for which levitation is producing overabundances of Fe-peak elements for the slow-rotating Fm stars (T98b).

The results from T98a, T98b, and R98 are taken directly from the articles, using a digitalization of Figures 11 and 12 from T98b, Figure 1 from T98a, and Figures 1 and 7 from R98 (the original data for the structure, acceleration, and monochromatic opacities were not available to us).

TABLE 6
COMPARISON OF γ(C) OBTAINED WITH OPAL AND OP DATA (NEW AND OP5)

log T	log ρ	log $T_{\rm eff}$	r/R_*	log $\gamma^{\rm NEW}$	log $\gamma^{\rm OPAL}$	log $\gamma^{\rm OP1}$	$\delta\gamma_1/\gamma$ (%)	$\delta\gamma_2/\gamma$ (%)	$\delta\gamma_3/\gamma$ (%)
6.0.....	−1.5	3.762	0.7146	2.621	2.625	2.585	−0.9	8.0	−8.8
6.0.....	−2.0	3.762	0.7146	2.526	2.535	2.496	−2.1	6.7	−8.6
6.0.....	−2.5	3.762	0.7146	2.420	2.424	2.396	−0.9	5.4	−6.2
6.0.....	−3.0	3.762	0.7146	2.322	2.343	2.299	−5.0	5.2	−9.6
6.3.....	−0.6	3.762	0.7146	2.089	2.060	2.020	6.5	14.7	−8.8

NOTES.—The effects of momentum transfer to the electron are taken into account. For this comparison, $\delta\gamma_1/\gamma = (\gamma^{\rm NEW} - \gamma^{\rm OPAL})/\gamma^{\rm NEW}$, $\delta\gamma_2/\gamma = (\gamma^{\rm NEW} - \gamma^{\rm OP5})/\gamma^{\rm NEW}$, and $\delta\gamma_3/\gamma = (\gamma^{\rm OP} - \gamma^{\rm OPAL})/\gamma^{\rm OPAL}$.

TABLE 8

Comparison of the C Acceleration Obtained with OPAL and OP Data (NEW)

log T	log ρ	log $T_{\rm eff}$	r/R_*	log $g_{\rm rad}^{\rm NEW}$	log $g_{\rm rad}^{\rm OPAL}$	log $g_{\rm rad}^{\rm OP1}$	$\delta g_1/g$ (%)	$\delta g_2/g$ (%)	$\delta g_3/g$ (%)
6.0.....	−1.5	3.762	0.7146	4.030	4.058	3.887	−7	28	−32
6.0.....	−2.0	3.762	0.7146	3.607	3.648	3.494	−10	23	−30
6.0.....	−2.5	3.762	0.7146	3.074	3.138	3.000	−16	16	−27
6.0.....	−3.0	3.762	0.7146	2.495	2.565	2.460	−17	8	−21
6.3.....	−0.6	3.762	0.7146	3.273	3.266	3.064	2	38	−37

Notes.—The momentum transfer to the electron is taken into account, and the e^- scattering has been removed from the carbon monochromatic opacities using the OP data. For this comparison, $\delta g_1/g = (g^{\rm NEW} - g^{\rm OPAL})/g^{\rm NEW}$, $\delta g_2/g = (g^{\rm NEW} - g^{\rm OP1})/g^{\rm NEW}$, and $\delta g_3/g = (g^{\rm OP1} - g^{\rm OPAL})/g^{\rm OPAL}$.

The results for the Rosseland mean opacities are presented in Figure 2. There are four panels representing the percentage difference in $\kappa_{\rm R}$ for the four stellar models studied.

3.3.2. *Results*

The OPAL $\kappa_{\rm R}$ values have been calculated using the tables and the routines provided on the OPAL Web site.[5] The results for the accelerations for the solar model at 4.57 Gyr are presented in Figure 3. We have plotted the ratios $g_{\rm rad}/g$ using OP and OPAL data for several elements, where g is the gravity. There is a maximum difference of 10% in $\kappa_{\rm R}$, but the difference in $g_{\rm rad}$ rises to 60% for Fe and up to 200% for C between the accelerations calculated with the new OP data and the data extracted from T98b, in the sense that the OP values are smaller. For physical conditions appropriate for the base of the solar convection zone, the difference [defined as (NEW − OPAL)/NEW] is 20% for Fe and 150% for C.

[5] See http://www-phys.llnl.gov/Research/OPAL/.

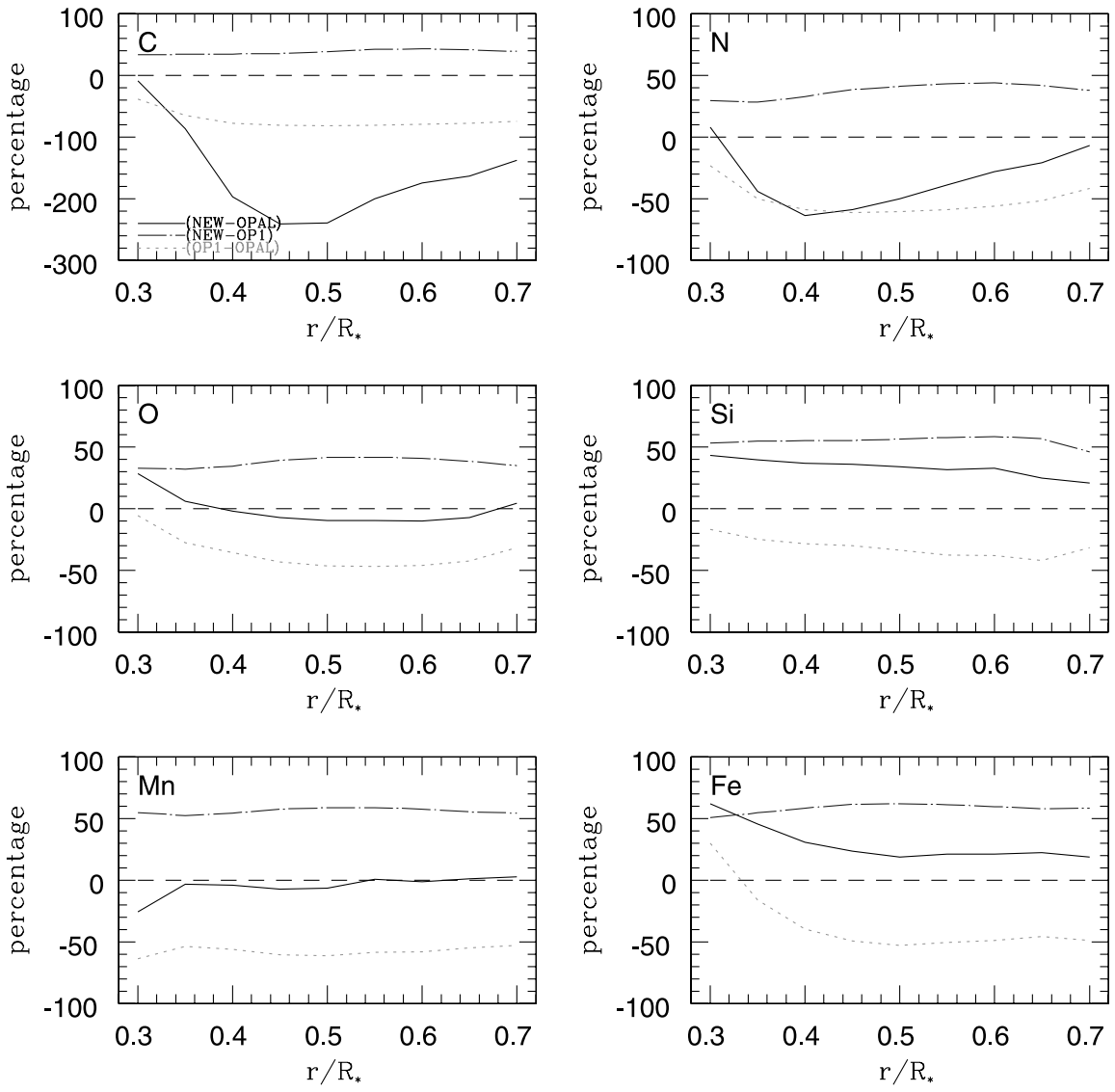

Fig. 3.—Percentage difference in acceleration for the solar model. [*See the electronic edition of the Journal for a color version of this figure.*]

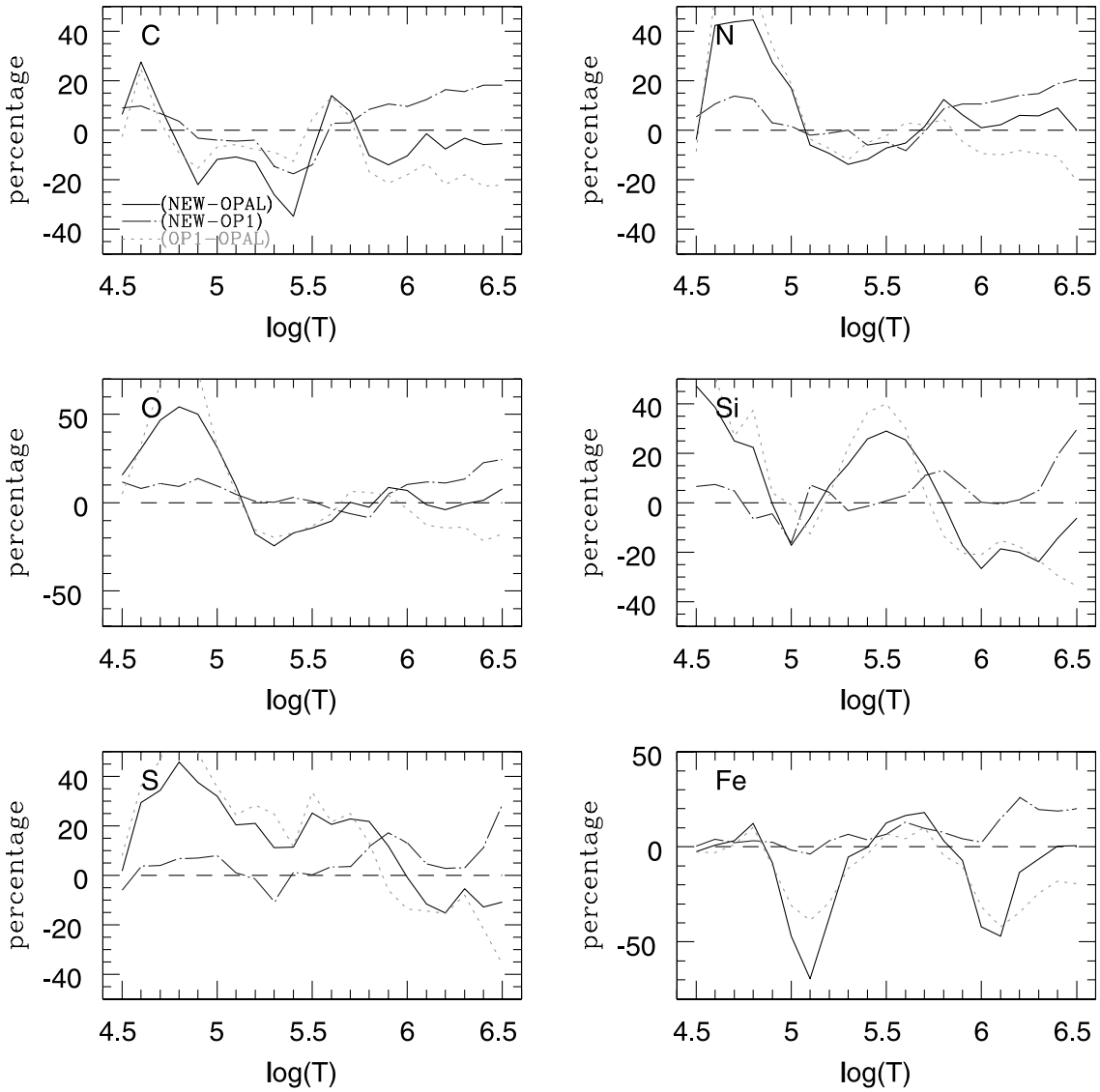

FIG. 4.—Percentage difference in acceleration for $T_{\rm eff} = 10{,}000$ K and $\log R = -3$. [*See the electronic edition of the Journal for a color version of this figure.*]

The accelerations for the second model, with $T_{\rm eff} = 10{,}000$ K and $\log R = -3$, are presented in Figure 4. The Rosseland means agree within 15%, and the radiative accelerations agree within 50%.

Figures 5 and 6 give the results for the next two models ($M = 1.3$ and $1.5\,M_{\odot}$). The difference in the values of $\kappa_{\rm R}$ (Fig. 2) reaches a maximum of 35%, while the accelerations differ by less than 70%.

For all cases, regardless of the type of star or the region of the ρ-T plane explored, the differences in the Rosseland mean opacities between OP and OPAL data are much smaller than the disagreements between the corresponding accelerations. As described in § 3.1.1, $\kappa_{\rm R}$ cannot alone be held responsible for the large gap between $g_{\rm rad}^{\rm OP}$ and $g_{\rm rad}^{\rm OPAL}$. The combination of the discrepancies in $\kappa_{\rm R}$ and γ defines the differences in the radiative acceleration. The accelerations in the different stellar models show large discrepancies for most elements. The largest ones are found in the solar model.

3.3.3. *General Trends*

In § 3.1 we anticipated the differences in the acceleration for the elements heavier than carbon to be larger than those for carbon itself. For the last three cases ($T_{\rm eff} = 10{,}000$ K, $M = 1.3\,M_{\odot}$, and $M = 1.5\,M_{\odot}$) the results seem to roughly follow the trend (see Figs. 4, 5, and 6). However, the differences are well within 50%, with an rms of the difference smaller than 30%.

However, for the solar case, the differences in carbon accelerations are the largest. The differences for carbon range between a few percent to 250% through the solar structure, while all of the other elements have differences within 60% (the regions near the center, with small r/R_{*}, are uncertain because of the difficulties in digitizing this region). It is difficult to understand these results. Our direct comparison for carbon yielded a difference of 2% for point 5 of Table 1, where the physical conditions are similar to those at the base of the convection zone of the solar model. The results from T98b give a difference of 150% for similar physical conditions. In other words, our accelerations using OPAL data are smaller than those presented by T98b for similar conditions. The points are not exactly at the same ρ-T location, but it seems unlikely that this can explain such a large difference, because the changes of T and ρ are very small. We address this issue in the next section.

4. DISCUSSION

4.1. *Stellar Model Differences*

The first source of differences that we can think of is the stellar code itself. We digitized figures from the published papers and

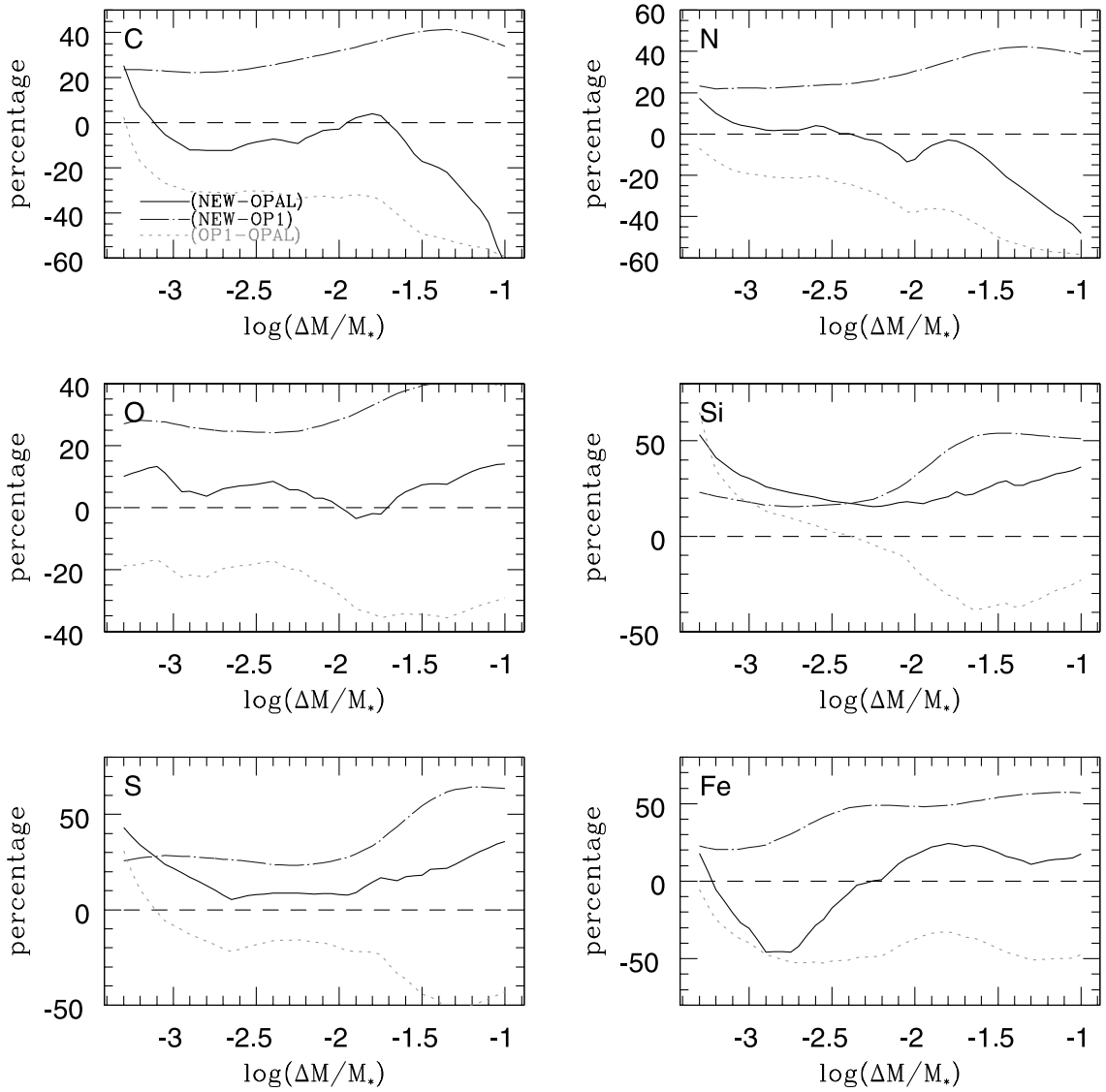

FIG. 5.—Percentage difference in acceleration for $M = 1.3\ M_{\odot}$. [*See the electronic edition of the Journal for a color version of this figure.*]

attempted to construct equivalent physical cases for our models. Our models were derived from a different stellar evolution code than the one used by T98a, T98b, and R98. In principle, differences in opacities and accelerations could therefore simply arise from differences in the structure of the models themselves (e.g., differences in ρ, T, or X_i). The total flux could also change the absolute scaling of the accelerations. The digitization process introduces errors. Even if the OPAL data were provided by the same author (C. Iglesias), it could be possible that our OPAL data differ from theirs. Finally, it is also possible that there are genuine differences in the calculated $g_{\rm rad}$ values that arise from errors in either calculation.

Modern solar models have very similar thermal structures for similar input physics, so we believe that structural differences are not an explanation for the differences in the solar case. When comparing our models with those of T98b (model H, Table 6), the base of the convection zone is at similar depth [$r/R_{\odot}$(model H, T98b) = 0.7176; $r/R_{\odot}$(present) = 0.7146], the temperatures are in very good agreement ($\log T_{\rm CZ}^{\rm T98b} = 6.3343$, $\log T_{\rm CZ}^{\rm pres} = 6.3360$), the central density and temperature are within 1%, and the composition is within a few percent at the surface. We also checked that a 10% difference in the composition does not produce any significant difference in the acceleration. The constraints on solar models are the strongest compared to other stellar models. The two models use similar input physics (the Krishna Swami T-τ relation is used for the atmosphere; the energy generation routines are the same, and both use the mixing length theory). The equations of state differ, but the effect is expected to be, and is, very small (for the center and the surface convection zone, ρ and T are within 1% in both models). Indeed, for the interior solar conditions, the gas can be assimilated to a fully ionized ideal gas. It is very unlikely to have large differences in the structure. We calculated the partial derivatives of the acceleration at a few points to gauge the uncertainties due to the structure. The partial derivatives are calculated as simple differences: $\delta \log g_{\rm rad}/\delta \log X_i = \Delta \log g_{\rm rad}/\Delta \log X_i$, where X_i is T, ρ, or r/R_*. Two of the variables are kept constant while calculating the partial derivative.

At the base of the surface convection zone of our solar model, we have $(\delta \log g_{\rm rad}/\delta \log T)|_{\rho,r} = -5$, $(\delta \log g_{\rm rad}/\delta \log \rho)|_{T,r} = 0.5$, and $[\delta \log g_{\rm rad}/\delta(r/R_*)]|_{\rho,T} = -1.22$. This implies that a deviation of 20% in the temperature or a factor of 7 in density or a difference of 112% in the radius or flux is needed in the model in order to invoke the structure as the source of differences in the radiative acceleration. As we mentioned above, the differences are less than 1% for the temperature, less than 2% for the central

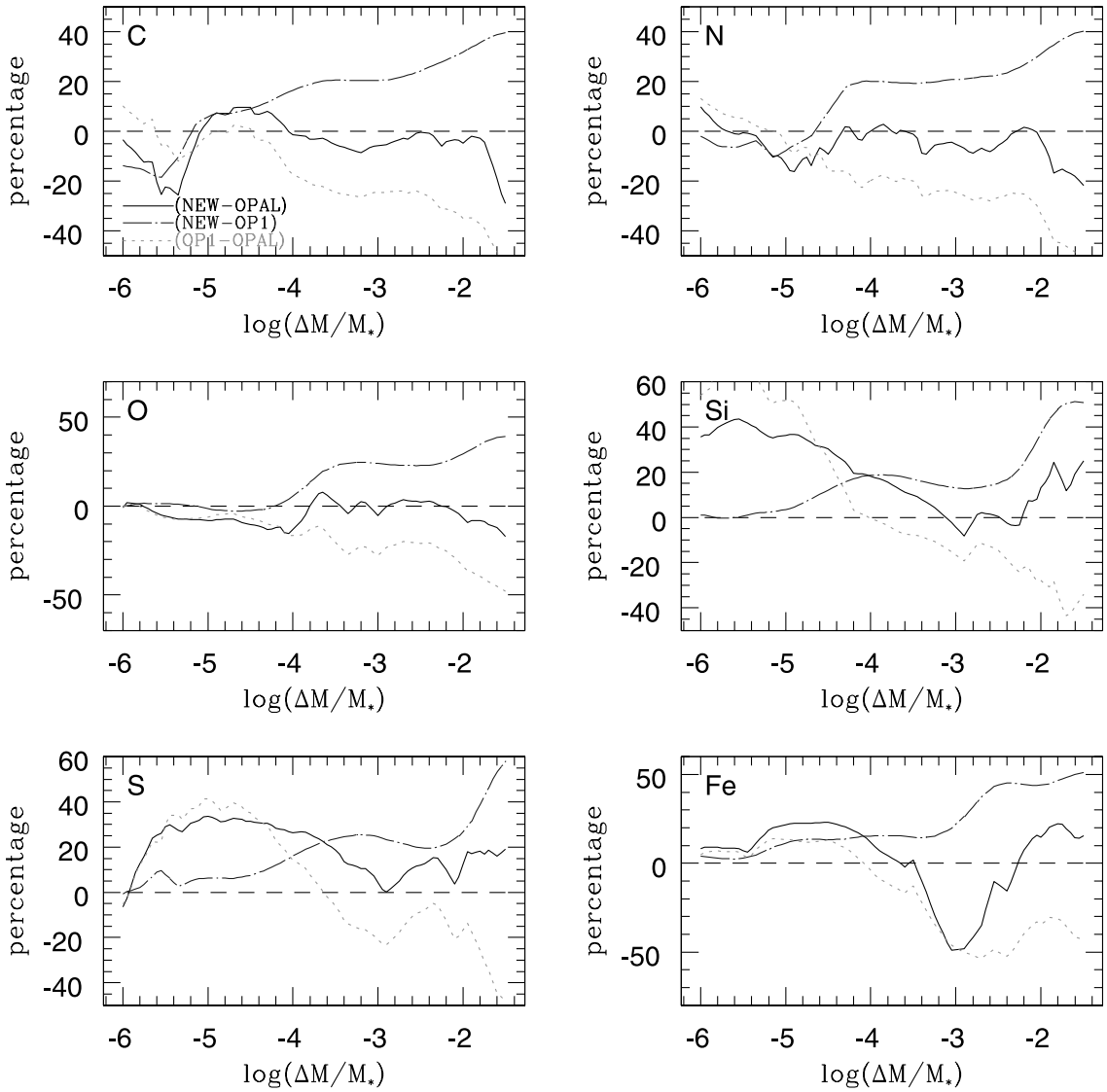

FIG. 6.—Percentage difference in acceleration for $M = 1.5\ M_{\odot}$. [*See the electronic edition of the Journal for a color version of this figure.*]

density, and less than 1% for the position of the base of the convection zone.

For the second model, the structure is just a vector defined identically in our model and the published one. It consists of a set of temperature points ($\log T = 4.3$–7.3) at a constant R ($\log R = -3$, with $R = \rho/T_6^3$ and $T_6 = T/10^6$).

For the two other models, the final model $T_{\rm eff}$ values are identical to those from T98a for a similar age. Thus, we expect the structures to be very similar; the effective temperature sets the convection zone depth, so the thermal structures should be similar at a fixed $T_{\rm eff}$ value.

Because the structure for the two last models is not as well constrained as the solar model and because the differences in the acceleration are not too large, it is a potential source of the differences between our calculation and the results from the literature. However, for the solar case, it is ruled out.

The composition is also not the right candidate, because it is equivalent to a solar composition in our model and in the three other models (the two last models are taken at the zero-age main sequence and by definition for model 2). For the solar case the composition does not change by more than 10%, and we checked that this does not affect the acceleration. The errors due to the digitization are at the level of 3%, which is measurable but much less than the differences that we are seeing.

The OPAL monochromatic opacities may be different from those used by the previous investigators. The data we received (C. Iglesias 2004, private communication) were recreated for five specific ρ-T conditions (Table 1). Despite the fact that we were able to reproduce Figure 3*a* of Iglesias & Rogers (1995), it is possible that the OPAL data used by Turcotte and others differ from ours. In the second case, in which the structures are identical by definition, we found differences in the OPAL Rosseland mean opacities. The extracted value from the plot (R98, Fig. 1) is $\kappa_{\rm R} = 3.45$ at $\log T = 6.0$ and $\log R = -3$, while our value is $\kappa_{\rm R} = 3.72$.

Finally, we should not exclude the possibility that the two results are really different for the same physical conditions, which could indicate an error in one or both calculations. We have been through the different possible sources of errors, and we do not speculate further on these results, given the number of inconsistencies. A direct comparison with the two sets of data would be more reliable, and we are expecting to be able to run it for other elements than carbon and for a large portion of the ρ-T plane. We will be glad to provide our data to allow others to run parallel comparisons.

4.2. *Further Discussion*

The frequency resolution used to sample the monochromatic opacities, as already mentioned by Seaton (1997, 1999), is another important source of possible differences in the accelerations. The calculations of κ_R and γ use a sampling technique (Seaton 1997; LeBlanc et al. 2000). All the cross sections are sampled at a specific frequency mesh and then integrated in order to calculate the Rosseland mean and γ. While a modest frequency resolution might be sufficient for the determination of κ_R, higher resolution is required for the acceleration. Indeed, as discussed in Seaton (1997), γ is much more sensitive to the frequency mesh than the Rosseland mean. The specific opacity uses a smaller number of lines than κ_R. If the frequency mesh is bigger than some line width, the sampling might miss some lines. On average, it has a small impact on the total opacity, given the large number of lines already included. However, it is more crucial for the specific opacity, which has less lines than the total opacity.

While both OP and OPAL agreed on the convergence of κ_R within 2% (Rogers & Iglesias 1992; Seaton et al. 1994) using 10^4 points over the range of significant frequency, using a constant mesh (u), Seaton (1997) compared the effect of varying the frequency resolution from $R = 10^4$ to 10^5 to 10^6 on γ. He showed that it could lead to a factor of a few difference in γ and varies depending on the element and the physical conditions. Seaton also addressed this issue in Appendix B of his 1999 article. While the frequency resolution used in OPAL data (constant-u mesh with 10^4 points over the whole frequency range) is adequate to determine with good accuracy the Rosseland mean opacity, it certainly limits the accuracy of the acceleration when the composition changes during the evolution calculations. The new OP data use an equally spaced mesh (v), which samples preferentially the region where f_ν is not too small (see Badnell et al. 2005). This increases significantly the accuracy of γ without requiring a prohibitive number of points. We have tested the results of the accelerations using 10^4 points in the v-mesh and compared with the acceleration using 10^5 points in the u-mesh. The results are in good agreement. We then expect more accurate accelerations to be derived from OP data than from OPAL data.

5. CONCLUSION

The phenomenon of radiative levitation can induce significant changes in the surface abundances of stars, and the underlying theory that predicts levitation of some elements is based on well-understood physics. However, quantitative theoretical predictions rely upon subtle details in the radiative opacities, and it has been difficult to estimate the error induced by uncertainties in the atomic physics and equation of state. The availability of two independent theoretical sources for opacity data (OP and OPAL) therefore provides an important test of systematic errors and their potential impact on this problem, as well as other aspects of the theory of stellar structure and evolution.

We have calculated the radiative accelerations using the updated OP opacities, which include all contributing inner shell processes. The impact on g_{rad} is important and generates an increase by up to 80% compared to the data without the inner shell. The light elements are less affected than heavy species. The former change by up to 40%, while the latter are affected to an 80% level. It is important to note that the difference in accelerations was significantly larger than the difference in the Rosseland mean opacities; we have traced through the interplay of factors that is responsible for the increased sensitivity of radiative acceleration computations to changes in the underlying atomic physics relative to the mean opacity.

In the case of carbon, we were able to directly compare the OP and OPAL data for some cases. We found that the accelerations derived from the new OP data differ by less than 17% compared to the accelerations derived from OPAL data. As expected, we found larger differences for heavier species in indirect comparisons with published literature values, ranging from 10% to 70%, than the OPAL ones, depending on the element and the physical conditions.

However, these indirect comparisons also gave larger differences for C than the ones that we computed directly. In other words, our reconstruction of the C accelerations from the OPAL data differ from the published accelerations calculated using OPAL data, in the sense that our OPAL accelerations are smaller. For the case that can be compared most directly (our solar case), the differences were 2%, while the differences with the published work reach 150%.

There are a variety of possible explanations. We had to digitize plots published for sample physical cases, and both digitization errors and differences in the published thermal structure relative to our models could contribute to the discrepancies. There could also be systematic differences in the accelerations for the same physical conditions, which should be explored. In our view it would be most fruitful to simply perform a direct comparison rather than to speculate. Until such a direct comparison can be made, it is reasonable to infer that different sources for opacities can produce differences at the factor of 2–5 level in the accelerations. We do note that the differences found for other elements were larger than the discrepancies between the two sets of carbon accelerations, suggesting that the relative trends (bigger differences for heavier species) are correct.

The new OP data are in better agreement with the OPAL data than was the case for the older OP data (Badnell & Seaton 2003; Seaton & Badnell 2004; Badnell et al. 2005), and by extension we expect that the accelerations will also be closer to those seen in the case of carbon. However, there are real differences in the relative opacities of different species between the OPAL data and the new OP data, and there are significant differences in the accelerations that we will discuss when we have access to the OPAL data.

There are two classes of direct astrophysical implications, one for the interpretation of stellar surface abundance anomalies and the other for tests of the opacities themselves. The differences in radiative accelerations have important consequences on the microdiffusion processes. The balance between thermal diffusion, gravitational settling, and radiative levitation is significantly modified. Lower values of g_{rad} could reduce the surface abundance anomalies, making it easier to reconcile the theoretical values with observations. It could also change the abundance profiles. Indeed, the depth at which one species is supported is directly linked to the balance between the three components of the diffusion processes. As a consequence, the Fe convection zone predicted in some F star models could lie deeper or even disappear. Levitation is only a perturbation in the solar case, and differences are unlikely to produce significant modification in the calibrated solar-like models. However, as the effective temperature increases, the effects increase as well. Therefore, theoretical errors need to be accounted for when comparing observations and theory.

More broadly, opacities play a crucial role in the theory of stellar structure and evolution. It has been difficult to establish the uncertainty in opacity calculations because of their complexity and the difficulty in obtaining direct measurements of opacity for plasmas under stellar interior conditions of temperature and density. The sensitivity of radiative acceleration calculations to the monochromatic opacities, however, may provide a useful test of the opacities themselves in cases in which the physical

situation is relatively simple. By extension, such comparisons will be useful for establishing the quality of opacity data across the entire stellar evolution field.

We would like to thank Carlos Iglesias for providing us with the carbon and total monochromatic opacity data from the OPAL project. We would also like to thank Michael Seaton, Carlos Iglesias, and Anil Pradhan for useful discussions. F. D. thanks Georges Alecian and Claude Zeippen for the fruitful discussions and collaborations during his stays in France. Part of this work was performed during stays by F. D. at the Observatoire de Paris, Meudon (France). F. D. is indebted to the INSU (CNRS, France) for support during those periods.

REFERENCES

Alecian, G. 1994, A&A, 289, 885
Alecian, G., & Artru, M.-C. 1990, A&A, 234, 323
Alecian, G., & LeBlanc, F. 2000, MNRAS, 319, 677
Alecian, G., Michaud, G., & Tully, J. 1993, ApJ, 411, 882
Badnell, N. R., Bautista, M. A., Butler, K., Delahaye, F., Mendoza, P., Palmieri, P., Zeippen, C. J., & Seaton, M. J. 2005, MNRAS, in press
Badnell, N. R., & Seaton, M. J. 2003, J. Phys. B, 36, 4367
Bahcall, J. N., & Pinsonneault, M. H. 1992, Rev. Mod. Phys., 64, 885
Bahcall, J. N., Pinsonneault, M. H., & Basu, S. 2001, ApJ, 555, 990
Bahcall, J. N., Pinsonneault, M. H., & Wasserburg, G. J. 1995, Rev. Mod. Phys., 67, 781
Behr, B. B., Cohen, J. G., & McCarthy, J. K. 2000a, ApJ, 531, L37
Behr, B. B., Cohen, J. G., McCarthy, J. K., & Djorgovski, S. G. 1999, ApJ, 517, L135
Behr, B. B., Djorgovski, S. G., Cohen, J. G., McCarthy, J. K., Côté, P., Piotto, G., & Zoccali, M. 2000b, ApJ, 528, 849
Chaboyer, B., Deliyannis, C. P., Demarque, P., Pinsonneault, M. H., & Sarajedini, A. 1992a, ApJ, 388, 372
Chaboyer, B., Sarajedini, A., & Demarque, P. 1992b, ApJ, 394, 515
Charpinet, S., Fontaine, G., Brassard, P., Chayer, P., Rogers, F. J., Iglesias, C. A., & Dorman, B. 1997, ApJ, 483, L123
Ferraro, F. R., Paltrinieri, B., Fusi Pecci, F., Rood, R. T., & Dorman, B. 1998, ApJ, 500, 311
Gonzalez, J.-F., LeBlanc, F., & Michaud, G. 1995, A&A, 302, 788
Grevesse, N., & Noels, A. 1993, Phys. Scr., T47, 133
Grundahl, F., Catelan, M., Landsman, W. B., Stetson, P. B., & Andersen, M. I. 1999, ApJ, 524, 242
Hui-Bon-Hoa, A., Alecian, G., & Artru, M.-C. 1996, A&A, 313, 624
Hui-Bon-Hoa, A., LeBlanc, F., & Hauschildt, P. H. 2000, ApJ, 535, L43
Iglesias, C. A., & Rogers, F. J. 1995, ApJ, 443, 460
———. 1996, ApJ, 464, 943
LeBlanc, F., & Alecian, G. 2004, MNRAS, 352, 1329
LeBlanc, F., & Michaud, G. 1995, A&A, 303, 166
LeBlanc, F., Michaud, G., & Richer, J. 2000, ApJ, 538, 876
Michaud, G. 1970, ApJ, 160, 641
Michaud, G., Richard, O., Richer, J., & VandenBerg, D. A. 2004, ApJ, 606, 452
Moehler, S., Heber, U., & de Boer, K. S. 1995, A&A, 294, 65
Richer, J., Michaud, G., Rogers, F., Iglesias, C., Turcotte, S., & LeBlanc, F. 1998, ApJ, 492, 833 (R98)
Richer, J., Michaud, G., & Turcotte, S. 2000, ApJ, 529, 338
Rogers, F. J., & Iglesias, C. A. 1992, ApJ, 401, 361
Sackmann, I.-J., & Boothroyd, A. I. 2003, ApJ, 583, 1024
Seaton, M. J. 1997, MNRAS, 289, 700
———. 1999, MNRAS, 307, 1008
Seaton, M. J., & Badnell, N. R. 2004, MNRAS, 354, 457
Seaton, M. J., Yan, Y., Mihalas, D., & Pradhan, A. K. 1994, MNRAS, 266, 805
Seaton, M. J., et al. 1995, The Opacity Project, Vol. 1 (Bristol: IoP)
———. 1997, The Opacity Project, Vol. 2 (Bristol: IoP)
Turck-Chièze, S., et al. 1998, in Proc. *SOHO* 6/GONG 98 Workshop, Structure and Dynamics of the Interior of the Sun and Sun-like Stars, ed S. Korzennik & A. Wilson (ESA SP-418; Noordwijk: ESA), 555
Turcotte, S., Richer, J., & Michaud, G. 1998a, ApJ, 504, 559 (T98a)
Turcotte, S., Richer, J., Michaud, G., Iglesias, C. A., & Rogers, F. J. 1998b, ApJ, 504, 539 (T98b)
VandenBerg, D. A., Richard, O., Michaud, G., & Richer, J. 2002, ApJ, 571, 487
Vauclair, S. 1998, Space Sci. Rev., 85, 71
Watson, W. D. 1970, ApJ, 162, L45